Separation and Purification Technology 347 (2024) 127644

Contents lists available at ScienceDirect

Separation and Purification Technology

journal homepage: www.elsevier.com/locate/seppur

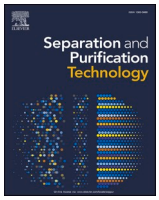

Investigating hydrodynamic cavitation as an efficient means for removal of per- and polyfluoroalkyl substances from solution

Shervin Kabiri [a,*], Mehdi Jafarian [b], Divina A. Navarro [c], Catherine P. Whitby [d], Michael J. McLaughlin [a]

[a] School of Agriculture, Food and Wine, The University of Adelaide, Waite Campus, PMB1, Glen Osmond, South Australia 5064, Australia
[b] School of Mechanical Engineering, University of Adelaide, Adelaide 5005, Australia
[c] CSIRO Land and Water, PMB 2, Glen Osmond, SA 5064, Australia
[d] School of Natural Sciences, Massey University, Palmerston North 4410, New Zealand

ARTICLE INFO

Keywords:
Per- and polyfluoroalkyl substances
PFASs
Separation
Foam
Colloidal gas aphrones
High shear

ABSTRACT

With nearly five decades of per- and polyfluoroalkyl substances (PFASs) being associated with firefighting and industrial activities, these compounds inevitably accumulate in both ground and surface water. PFAS contamination in water has emerged as a significant environmental and public health concern, particularly perfluorooctanesulfonic acid (PFOS), which is often found in higher concentrations compared to other PFAS and has more pronounced adverse health effects. Addressing PFAS contamination requires treating large volumes of water, making technologies that rapidly separate and concentrate PFASs highly favoured. The strong surface activity of PFAS, such as PFOS, enables them to generate colloidal gas aphrons (CGAs) during high shear mixing of their aqueous solutions, where PFASs can be separated and collected as foam. This study aims to evaluate the effectiveness of high shear mixing in separating PFOS from solution, leveraging its accumulation at air–water interfaces. High shear-assisted PFOS separation was tested by varying parameters like rotational speed (4000 to 10,000 rpm), mixing time (30 s to 30 min), and the effect of electrolytes. Results showed greater PFOS separation in the presence of electrolytes, particularly monovalent cations like Na^{+}, compared to divalent cations such as Ca^{2+}, due to the creation of more stable CGAs with smaller sizes. At a mixing rate of 6000 rpm, 85 % of PFOS was removed in 30 s from a highly contaminated PFOS solution (10 mg/L), with over 95 % separation after 5 mixing cycles. While high-shear mixing was efficient in PFOS separation from highly contaminated solutions it was less efficient for low-level contaminated solutions (less than 1 mg/L). These results suggest that hydrodynamic cavitation induced by high-shear mixing seems promising for enhancing the separation of PFOS from heavily contaminated solutions. This technique could serve as a standalone method or be integrated with other PFAS removal technologies to enhance the overall efficiency of PFAS removal from polluted water sources.

1. Introduction

Per- and polyfluoroalkyl substances (PFASs) constitute a group of exceptionally stable chemicals extensively employed in various industrial and household applications. The widespread use and disposal of PFASs have resulted in substantial environmental release, leading to pervasive contamination on a global scale [1]. As a result, PFASs have been detected in ground and surface waters, drinking water, soils and sediments around the globe. Moreover, the number of studies demonstrating the toxicity of PFASs to humans and animals, as well as their adverse effects on the environment, continues to increase. Recognising these concerns, both the United States Environmental Protection Agency (USEPA 2019) [2] and the Australian National Environmental Management Plan (NEMP 2020) [3] have established remediation goals for contaminated waters, setting acceptable levels at parts per trillion for some PFASs, which is lower than the cleanup standards established for other organic pollutants [4].

PFAS molecules are made up of a chain of linked carbon and fluorine atoms (CF_2) with different CF_2-length and a variety of functional head groups with either anionic, cationic or zwitterionic properties which can complicate their removal from different matrices [5]. Furthermore, due to their thermal and chemical stability, many of the *in-situ* or *ex-situ*

* Corresponding author at: School of Agriculture, Food and Wine, The University of Adelaide, Waite Campus, PMB1, Glen Osmond, South Australia 5064, Australia.
E-mail address: Shervin.kabrir@adelaide.edu.au (S. Kabiri).

https://doi.org/10.1016/j.seppur.2024.127644
Received 18 March 2024; Received in revised form 11 April 2024; Accepted 22 April 2024
Available online 24 April 2024

water treatment technologies have been found to be ineffective at removing them from water. Considering different water treatment technologies, the adsorption of PFASs on commercially available activated carbon or ion exchange resins is one of the preferred methods to remove PFASs from water, especially long-chain PFASs [6]. However, a disadvantage of this approach is the resulting residue from the adsorption process, including the spent activated carbon or resins, which must be treated for proper disposal or regenerated for further use [7]. For instance, the conventional practice of disposing of spent activated carbon or ion exchange resins in landfills involves high costs and potentially poses an additional risk of human exposure to PFASs through landfill leachates if not managed properly in well-designed landfills [8,9]. While spent activated carbon can undergo regeneration through thermal destruction, this method can be costly due to its high-temperature/energy requirements [10,11]. Regenerating ion exchange resins, on the other hand, necessitates a mixture of solvents and salts, introducing a new challenge in managing the regenerated solution [12]. Other PFAS removal techniques from contaminated water such as reverse osmosis, are complex and potentially expensive to install and maintain, particularly due to costs associated with membrane fouling [13,14]. Destructive technologies such as hydrothermal alkaline technique (HALT), thermal degradation/incineration, supercritical water oxidation or electrochemical oxidation can fully/partially degrade PFASs into harmless compounds. However, this technique is not economically viable for treating large volumes of contaminated water.

Recently, new technologies have been introduced based on the accumulation of PFASs at air–water interfaces that have been applied in the laboratory [15,16] and field scale [4] for groundwater and landfill leachate treatment [17]. Foam fractionation is among these technologies that employs bubble columns. The surface active properties of PFASs lead to their accumulation at the bubbles' air–water interfaces. The bubbles (which are up to a few millimetres in diameter) are generated through the injection of air or N_2 at the bottom of the bubble column. The accumulated PFAS molecules at the surface of bubbles form a foam over the liquid surface as the bubbles rise through the water and the injected gas leaves the column. The concentrated foam layer is subsequently removed from the column, leading to a reduction in the concentration of PFASs in the water [17]. Foam fractionation appears to be economically viable and suitable for the separation of PFASs from aqueous systems as it relies solely on the established and simple bubble columns technology. Additionally, it can be designed in modular units enabling mobility based on demand. Moreover, it is eco-friendly and sustainable, mitigating the need for adsorbents or filter materials [4,17]. Foam fractionation has demonstrated a high removal efficiency for long-chain PFASs (>90 %). Nevertheless, it is less effective in removing short-chain PFASs (~20–70 %) and precursors (11–90 %) [18]. Recent research has shown that the addition of a cationic surfactant can enhance the removal of short-chain PFASs during foam fractionation [19,20]. Although foam fractionation is not primarily intended for the destruction of PFASs, it can effectively minimise the volume of water that requires further treatment. After the foam is collected, the concentrated PFAS solution can be destroyed by technologies such as hydrothermal alkaline treatments [21].

The key to efficient foam generation is aeration of the target solution to create a high air–water surface area, so better aeration by mixing at high speeds is proposed to create a larger air–water interface to enhance PFAS adsorption. However, mostly variations of bottom-up aeration (bubbling) have been reported to date [19,20]. Stirring the reaction vessel (mechanical mixing to aerate using shear forces) is entirely unexplored in the context of PFAS separation. In this project, we propose to trial the use of high shear mixing (HSM) to efficiently mix and aerate PFAS-contaminated solution. High-shear mixing typically results in the formation of bubbles (CGAs) within the liquid due to hydrodynamic cavitation and hence it can be employed for the separation of PFASs from water. Removal of pharmaceutical pollutants from wastewater through a venturi, as cavity generator [22], and a hydrodynamic cavity generator [23] has been studied. Furthermore, high shear mixers have been applied in protein and biological separation [24,25], mineral processing [26,27], water purification as well as soil remediation [28–31]. The phenomenon of hydrodynamic cavitation occurs when the local static pressure in a liquid falls below the vapour pressure of the liquid, forming vapour-filled cavities or bubbles [32]. This pressure drop can occur due to the variation in the velocity profile, caused by high-speed passage of the liquid through a constriction, such as an orifice plate or venturi pipe, or the use of a high speed rotary blade [33]. Applying an adequately high shear rate to a surfactant solution can create colloidal gas aphrons (CGA) comprised of gas bubbles with a typical size distribution of 10 – 100 μm that are stabilised by multiple layers of the surfactant [34,35]. On this basis, the idea here is to use a high-speed mixer to form CGAs in a PFAS-contaminated water. The CGAs rise through the liquid to form a foam that can be extracted and hence lead to effective separation of PFASs from water. This method can create a large interfacial surface area due to the relatively small bubble size, contributing to the adsorption of surface-active compounds like PFASs or formation of CGAs made of PFASs due to their surfactant nature. This is advantageously in contrast to existing bubble column foam fractionation technologies with relatively larger bubbles. The formation of CGAs will be critical in the separation of PFASs via high shear mixing. The CGAs formed exhibit a range of properties that are influenced by the surfactant used in their formation and the method employed, including mixing speed and temperature. For example the addition of an electrolyte or polymer to the surfactant solution, can reduce the size of CGAs and increase their stability [35,36]. Similarly, the size of CGAs and their stability can be influenced by mixing speed and solution temperature [37,38].

HSM can potentially offer several benefits for remedial applications, including availability in different scales, portability, energy-efficiency, cost effectiveness, and ease of fabrication, operation and maintenance. Therefore, the feasibility of HSM for removing PFASs from solution through formation of CGAs warrants investigation. This study presents the results of a proof-of-concept experiment using a HSM that is commercially available to concentrate and remove PFASs from a highly contaminated solution. The separation of PFASs is based on their surfactant properties and the ability to create CGAs containing a gaseous core and a thin multi-layered aqueous surfactant shell. This study assessed the effect of solution mixing speed, temperature, PFAS type and concentration on the separation of PFASs from contaminated solutions. Since HSMs are simple to operate, portable and only require a mixing vessel for operation, they can be used for PFASs removal from water at different scales and in diverse environments. To the best of our knowledge this is the first study to demonstrate the separation of PFASs from water by HSM.

2. Materials and methods

2.1. Chemicals and materials

Heptadecafluorooctanesulfonic acid potassium salt ($CF_3(CF_2)_7SO_3K$), perfluorooctanoic acid −PFOA ($CF_3(CF_2)_6$ COOH) and perfluorohexasulfonate −PFHxS ($CF_3(CF_2)_5SO_3H$) solids used to prepare highly concentrated PFASs stock solutions were all purchased from Sigma Aldrich. Sodium chloride (NaCl, AR grade) and calcium chloride ($CaCl_2{\cdot}2H_2O$, AR grade) were also purchased from Sigma Aldrich. PFAS standards and isotopically labelled standards in methanol Perfluorobutanesulfonate ($13C_3$-PFBS), perfluoro-1-hexanesulfonate ($18O_2$-PFHxS), Perfluoro-butanoic acid ($13C_4$-PFBA), perfluoro-pentanoic acid ($13C_3$-PFPeA), perfluoro-hexanoic acid ($13C_4$-PFHxA), perfluoroheptanoic acid ($13C_4$-PFHpA), perfluoro-octanoic acid ($13C_4$-PFOA), perfluoro-nonanoic acid (13C5-PFNA), perfluoro-decanoic acid ($13C_2$-PFDA) and sodium perfluoro-1-octanesulfonate ($13C_8$-PFOS) were purchased from Wellington Laboratories Inc (Guelph, Ontario, Canada). These were used to prepare calibration standards and as internal

standards for PFAS analysis.

2.2. High-shear-assisted apparatus

A bench scale L5M-A batch mixer (Silverson, UK) was used to generate high shear within the PFAS solution. The mixer contained a stainless-steel blade with a cover around it with a mixing rate up to ~10,000 rpm. An acrylic vessel with an inner diameter of 74 mm and a height of 315 mm was used for all experiments (Fig. 1). The mixing head was placed in the centre of the vessel and 25 mm above the bottom. A screen that consisted of 5 holes of 10 mm diameter surrounding the mixing blade was used in all experiments. The confined space between the rotating blade and the stagnant screen (cover/casing) enables a higher shear, facilitating the generation of bubbles.

During mixing, the rotating agitator (rotor) also functions as a centrifugal pump, drawing water from the gap around the rotating shaft and expelling it through the screen holes. This creates a circulating flow within the container, drawing the liquid upwards from the bottom of the vessel. When the vessel has a cylindrical shape, vortexing can occur on the side of the mixing impeller which can introduce air into the solution. The air is sucked into liquid by the pressure difference. The air dispersion into the bulk liquid will increase as the mixing speed increases.

2.3. PFAS separation experiments

All experiments were conducted with 400 mL of PFOS solution with a concentration of 10 mg/L, except for the cases described below. The foam created in the experimental vessel during mixing the PFAS solution at a given time or mixing speed, is depicted in Fig. 1. As soon as the mixing finished, the foam floated to the top of the solution. Samples of the foam and the solution were taken from the top and bottom of the vessel, respectively, for PFAS analysis. The change in volume of the solution due to foam formation, as well as foam volume was recorded for each experiment and used for mass balance calculations.

The concentration of PFAS in wastewater from the photolithography process may exceed 1000 mg/L and PFAS concentration in the wastewater of aqueous film-forming foams can also be 3–6 g/L [15,39]. On the other hand the concentration of PFAS in ground and surface water, and landfill leachates is usually in 10–1000 μg/L ranges [19,40]. Therefore, different ranges of PFAS concentration were used in this study but the focus was mostly on highly contaminated solution to be able to proof the main concept of this study.

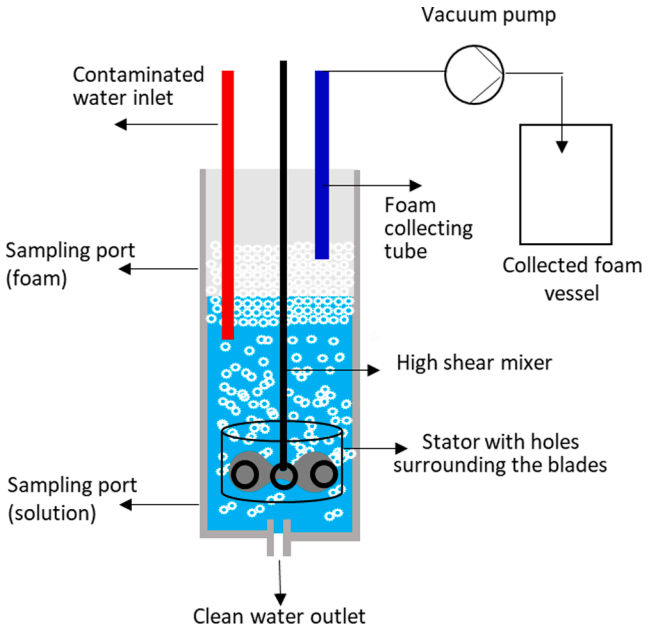

Fig. 1. Schematic diagram of the high-shear mixing apparatus.

The effect of shear rate, mixing time, PFAS concentration and type, and the presence of different salts were investigated. To investigate the effect of shear rates, a PFOS solution (10 mg/L) in MQ water was mixed at different rates (2000, 4000, 6000, 8000 and 10,000 rpm) for 4 min as the variations in rotational speeds can impact both the energy consumption of the instrument and the resulting shear force. Energy consumption plays a role in the economic feasibility of the technology, while shear force influences the formation of CGAs including bubble size and stability. At the same time, the effect of ionic strength on PFOS separation was investigated by mixing a PFOS solution (10 mg/L) made in 10 mM NaCl solution at different mixing rates (2000 to 10,000 rpm).

The effect of mixing time on PFOS separation was examined by mixing the solution (15 mg/L) at 6000 rpm under different time frames (30 s, 2, 4, 8, 16, and 32 min). As high shear spinning can create high energy during the mixing, the temperature of the solution was also monitored during all the experiments. The influence of initial PFOS concentration was investigated by using solutions containing 100 μg/L, 1 mg/L and 10 mg/L PFOS. At the same time, the effect of different salts was investigated by adding 10 and 50 mM NaCl, 4 mM and 10 mM $CaCl_2$ to the separation vessel. The effect of PFAS CF_2-chain length and the functional head group was also investigated by diluting an aqueous film-forming foam (AFFF) solution containing a mix of PFASs to have a solution concentration with $\sum$PFAS = 1 mg/L.

A mixture of PFOS, PFOA and PFHxS solution with the concentration of each PFASs adjusted to 10 mg/L was mixed in the presence of 10 mM NaCl for 1 min at 6000 rpm to investigate the effect of PFASs carbon-chain length and head group on removal using HSM. This experiment was repeated over 5 shear cycles. The foam was removed with each cycle, then the remaining solution was mixed for 1 min at 6000 rpm to investigate the removal of different PFASs. Microscopic photos of foams were taken using a Nikon Ni-E optical microscope to enable the characterisation of the CGAs formed.

2.4. PFAS analysis

Samples of the collected foam or solution were diluted with water and then 50 % methanol and prepared with 20 ug/L internal standard for PFAS analysis. Samples were analysed for PFAS concentration using a Thermo Scientific TSQ Altis triple-quadrupole mass spectrometer equipped with Thermo Scientific UltiMate 3000 HPLC system. A 10 μL sample was injected to a Phenomenex Kinetex 2.6 μm C18 (100x2.1 mm) column which was maintained at 40 °C. Two mobile phases of 5 mM ammonium formate (NH_4HCO_2) and methanol at a flow rate of 0.25 mL/minutes were used while a gradient program was used for PFAS analysis. The gradient elution started with 10 % methanol which was held on for 2 min, after which increased to 20 % methanol in 4 min, then 98 % methanol in 6 min. This condition was kept until 12.4 min then the mobile phase was immediately switched to 10 % methanol, finishing with a total run time of 15 min. Quantitation was based on internal standard calibration where analogous isotopically labelled PFAS are available. The limit of quantification for both PFOS, PFOA and PFHxS was 0.5 μg/L while for other PFASs were varied from 0.2 to 0.5 μg/L.

2.5. Calculations and statistical analysis

PFAS separation from the solution was calculated using the equation;

$$\%separation = \frac{C_{total} - C_e}{C_{total}} \times 100 \quad (1)$$

where C_e is PFAS concentration (mg/L) in the solution after mixing and foam removal and C_{total} is initial concentration of PFASs (mg/L). Mass balance was calculated based on equation (2);

$$Massbalance = \frac{(C_e{*}V_e + C_f{*}V_f)}{C_{total}{*}V_{total}} \quad (2)$$

where C_e is PFAS concentration (mg/L) in the solution after mixing and foam removal, V_e (L) is the volume of solution left in the vessel after removing the foam, C_f (mg/L) is PFAS concentration in foam and V_f (L) is the volume of collected foam, and V_{total} (L) is the initial volume of the solution before mixing.

IBM SPSS statistical software was used for analysis of variance (ANOVA). Multiple comparisons of means were conducted using the LSD test when the ANOVA indicated significant differences. The level of significance was set at $p \leq 0.05$.

3. Results and discussion

3.1. Effect of shear rate and electrolyte concentration on PFOS separation

Mixing at different rates decreased the PFOS concentration to varying degrees in solutions with no electrolyte (Fig. 2a). No significant differences were observed in the PFOS separation among solutions stirred at rotational speeds ≤ 8000 rpm ($p \leq 0.05$). The most substantial PFOS separation, representing the lowest concentration in the remaining solution, occurred at 10,000 rpm, where 42.7 % of the initial PFOS mass was effectively removed (Fig. 2b). The increased separation efficiency at 10,000 rpm can be attributed to the enhanced stability of CGAs, evident in the prolonged half-life of CGAs achieved by raising the rotational speed. This facilitates the efficient harvesting of PFOS as a foam, enabling effective separation from the solution. Similar observations of increased stability of CGAs produced from various surfactants have been reported by others. [38].

The presence of NaCl (electrolyte) in the solution led to a significant improvement in the separation efficiency and decrease in PFOS concentration in the remaining sample, in contrast to the solution without NaCl (Fig. 2a). Consistent findings by others support this, where the addition of electrolytes, such as NaCl, resulted in greater PFAS separation compared to experiments conducted without electrolytes [15,16]. High shear, coupled with the presence of the surfactant (PFOS), facilitated the generation of CGAs in the solution, irrespective of the presence of NaCl. However, NaCl did influence both the quantity and stability of CGAs (Figure S1, SI). In the presence of NaCl, CGAs exhibited significantly smaller sizes, and more foam was generated. The addition of NaCl contributed to a decrease in the surface tension of the PFAS solution [19], enhancing foamability, CGA stability, and half-life [35,37]. Electrolytes, such as NaCl, may also reduce hydrophobic attraction between bubbles by generating repulsive hydration forces [35,41]. Additionally, reducing the size of gas bubbles due to presence of electrolyte such as NaCl can enhance their negative surface charge, increasing electrostatic repulsion and overall stability. This is in agreement with the findings of Meng et al. [15] who demonstrated that the volume of foam and stability of air bubbles increases in the presence of NaCl. Therefore, the reduction in bubble size and enhancement of PFOS foam stability holds the potential to increase PFOS separation during the separation process.

Mass balances between 91 to 106 % were achieved for both NaCl-free and NaCl-containing solutions at rotational speeds of 4000 and 6000, but the mass balance dropped to 60–66 % for higher rotational speeds. Higher rotational speeds can generate smaller CGAs (Fig. 3c-f), and there is a possibility that some PFOS may have been removed from the mixing vessel as aerosol. Nguyen et al. [42] showed that during the aeration of PFAS-contaminated wastewater, PFAS can exit the aeration vessel as aerosol. Additionally, they observed less mass recovery at high aeration rates compared to low aeration rates. Similarly, while HSM can create smaller bubbles compared to aeration using gas bubbles, at high rotational rates, some of these bubbles may exit the separation vessel as aerosol that can lead to variability at mass balance. However, more studies are required to confirm this.

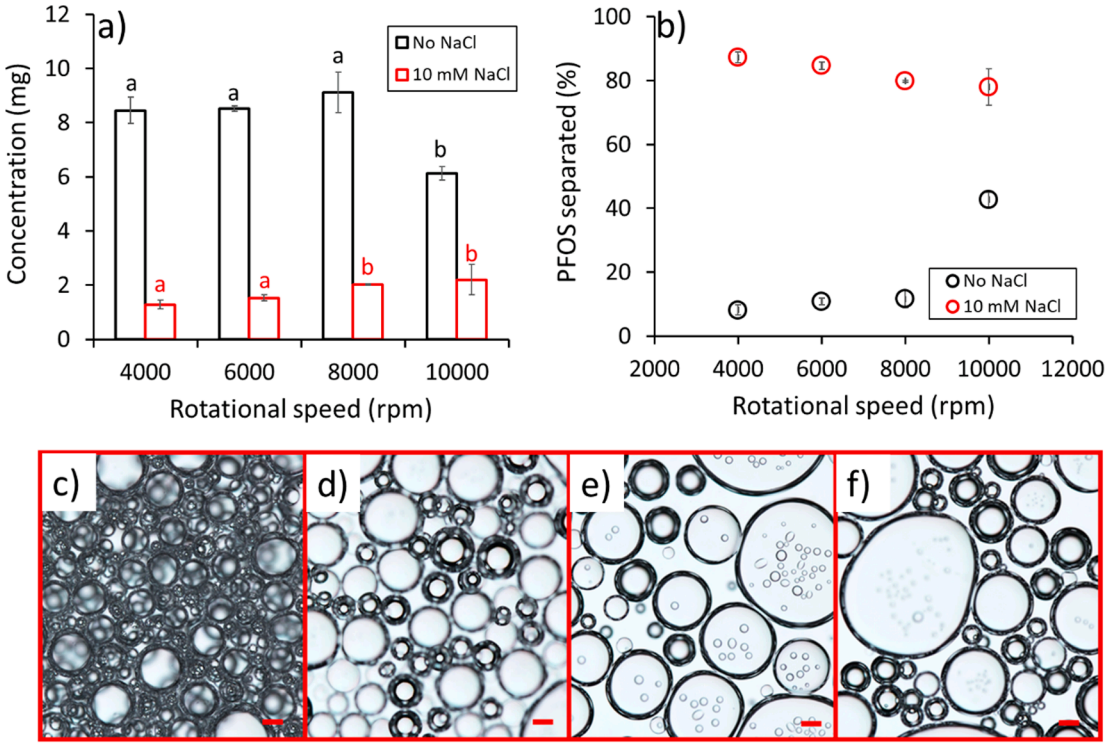

Fig. 2. (a) The mass of PFOS remaining in solution (mg) after mixing a contaminated solution (containing 10 mg PFOS) with or without NaCl at different rotational speeds for 4 min and (b) percentage of PFOS separated from the solution at different speeds, and microscopic images of foams from different positions that created at 4000 rpm (c and d) in the presence of electrolyte (10 mM NaCl) and (e and f) no electrolyte (no NaCl). Scale bars represent 100 μm. Error bars represent standard deviation of n = 3. (The statistical differences between the same treatments with different rotational speeds are represented by letters 'a' and 'b', where treatments with no significant differences are assigned the same letter, and those with significant differences are assigned different letters.).

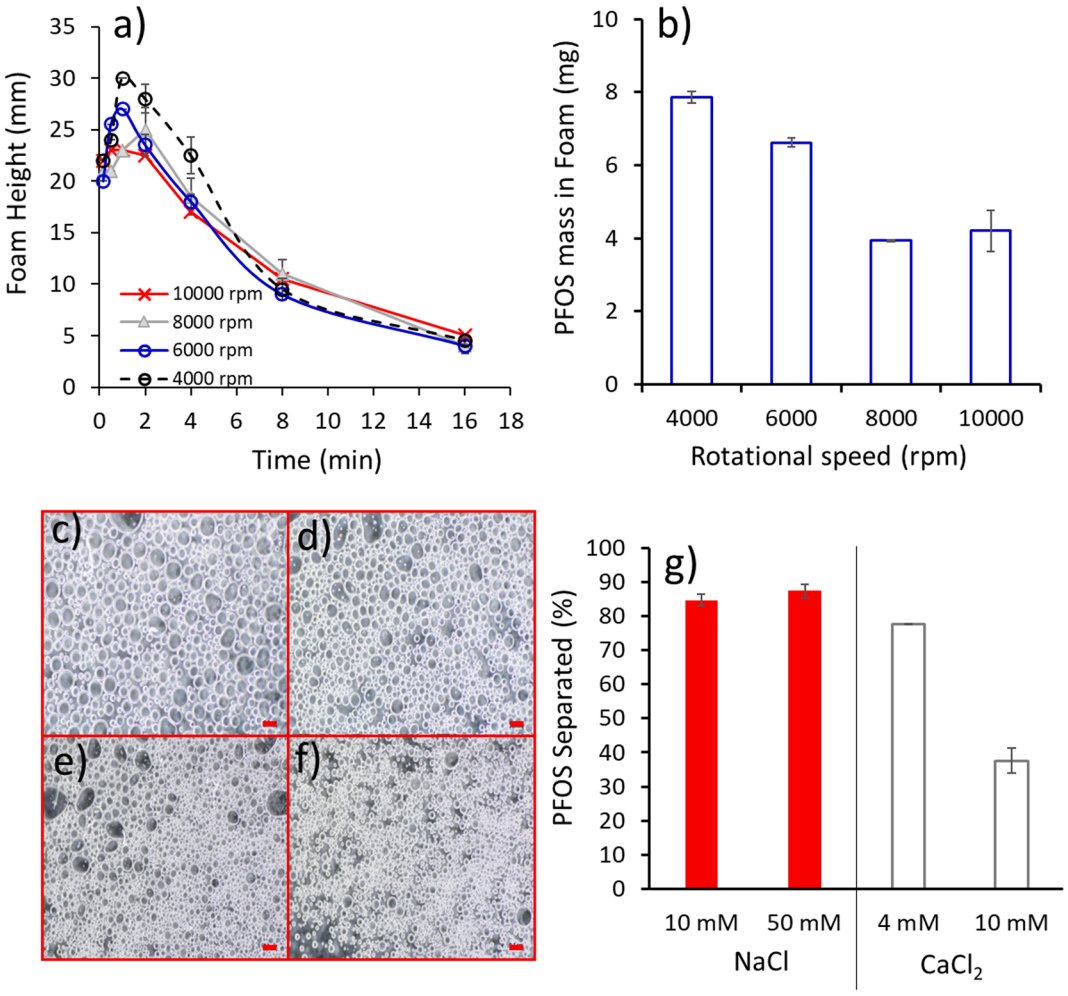

Fig. 3. (a) Foam height on top of solution at different time intervals after mixing stopped as a function of mixing rates, (b) Mass of PFOS measured in the collected foam after mixing at different mixing rates for 4 min (the initial PFOS mass in the solution was 10 mg), (c-f) Microscopic images of the foam collected from the top of the vessel after mixing stopped. These were taken for solutions mixed at 4000 (c), 6000 (d), 8000 (e), and 10,000 (f) rpm (The red line corresponds to 100 μm), and (g) PFOS separation efficiency in the presence of different electrolytes. Error bars are representing standard deviation of n = 3.

The most substantial reduction in PFOS concentration within the PFOS-NaCl solution occurred using 4000 rpm, resulting in 85 % removal of the pollutant mass (Fig. 2b). Notably, there was no significant difference in PFOS separation between mixing rates of 4000 and 6000 rpm ($p \leq 0.05$) (Fig. 2a), with nearly 80 % of the initial PFOS removed using 10,000 rpm. The observed decrease in PFOS separation with increasing mixing rates can be attributed to variations in CGA sizes and the quantity of foam generated. At 4000 and 6000 rpm, the foam height and volume were notably greater compared to other mixing speeds (Fig. 3a and Figure S2, SI), correlating with the mass of PFOS in the collected foam (Fig. 3b).

After mixing stopped, foams generated by HSM initially increased in height and then slowly degraded (Fig. 3a). Increasing the mixing rate led to a reduction in CGA size and foam volume measured during the initial 3 min of foam formation on top of the separation vessel Fig. 3a and c). The presence of bubble swarms in the liquid pool can influence interactions between bubbles, affecting the hydrodynamics of the liquid flow around them and altering the shape and interfacial behaviour of the bubbles [43]. Fast-moving bubbles in a swarm can decrease movement of adjacent bubbles regardless of their size, and a large population of fine bubbles can also decrease the rise velocity of all bubbles. This may explain the lower concentration of PFOS in the foam with increasing mixing speed (Fig. 3b) [44]. This may explain the lower concentration of PFOS in the foam with increasing mixing speed (Fig. 3b). Observation of foam formation and collapse across all solutions confirmed their correlation with CGA size, influenced by different mixing speeds.

While the addition of the electrolyte (10 mM NaCl) increased foam stability and PFOS separation from solution, increasing the NaCl concentration up to 50 mM NaCl did not increase the PFOS separation significantly (Fig. 3g). Meng et al. [15] also showed that PFOS elimination by foam fractionation increased from a solution by increasing NaCl concentration until a certain concentration of NaCl and remained constant afterwards. However, Buckley et al. [19] reported greater removal of PFOS by foam fractionation at 100 mM NaCl compared to 10 mM NaCl. In our study, increasing the NaCl concentration to 50 mM produced a less stable foam with larger bubbles having irregular shapes where bubbles collapsed quickly taking the microscopic image difficult. This might be related to the decrease in the negative surface charge of the CGAs due to the enhanced shielding effect in the vicinity of the surface of CGAs enhancing bubble coalescence [45]. The presence of co-ions can cause screening of the electric double layer around the CGAs which can decrease the external negative electrostatic pressure around CGAs leading to pressure imbalance across the CGAs and their collapse [46]. While the addition of NaCl can decrease the surface tension of a PFOS solution and increase its foamability, increasing salinity can also decrease the foamability of the surfactant due to increased stability of micelles in the solution and their lower propensity for foaming [47]. Indeed, when NaCl was replaced with $CaCl_2$ (4 mM), PFOS separation

decreased to 77 %. By increasing the $CaCl_2$ concentration to 10 mM, PFOS separation was drastically decreased to 37 %. The foams created in the presence of $CaCl_2$ were much less stable than those formed in the presence of NaCl and collapsed in less than 2 min. Divalent cations can act as bridging cations between anionic PFOS molecules [48], resulting in the formation of aggregates that may supress foam formation.

The mass balance for these solutions varied greatly, ranging from 55 to 104 %, with the lowest mass balance observed for the solution with the highest concentration of $CaCl_2$. This could be related to underestimation of PFOS concentration, specifically in foam where greater concentrations of cations and PFOS are found. Steffens et al. [48] showed that PFOS concentration can be underreported when ionic strength is high and can be affected more by di-valent cations compared to mono-valent cations. However, Schaefer et al. [49] reported the minimal effect of 10 mM NaCl on PFOS air–water partitioning behaviour, which could explain better mass balance for the experiments with 10 mM NaCl compared to others.

3.2. Effect of mixing time

The concentration of PFOS remaining in the solution was relatively the same after mixing times ranging from 30 s to 32 min. For all mixing times studied, ~ 85 % separation was achieved (Fig. 4a and b). This shows that mixing the solution for longer times in the batch experiment has no effect on PFOS separation. However, the concentration of PFOS in the foam increased with mixing time up to 16 min, but decreased after mixing for 32 min. This could be related to the greater volume of foam formed after mixing for 32 min that could dilute the PFOS concentration within the foam. a greater foam height was observed at 32 min compared to other mixing times (Fig. 4c). That could be related to faster movement of CGAs after mixing for 32 min due to the increased temperature of the mixing solution (Fig. 4b). Zhang et al. [50] showed an increase in the rise velocity profiles of bubbles in the water and solutions of Triton X-100 surfactants as temperature increased from 6 to 40 °C. This was also observed in our experiments (Fig. 4b and Figure S3, SI), where the temperature of solutions mixed for 32 min increased by over 10 °C.

3.3. Effect of consecutive mixing and PFAS chemistry/concentration

Increasing the number of mixing events (cycles) progressively removed more PFASs from solution (Fig. 5). PFHxS and PFOA concentrations demonstrated a linear decrease with an increase in the number of cycles, while PFOS concentration exhibited an exponential decrease. Over 85 % of the initial PFOS mass was effectively removed in the first two cycles. Notably, in the presence of elevated PFHxS and PFOA concentrations, a 60 % decrease in PFOS separation was observed in the first cycle compared to experiments conducted under identical operational conditions but without PFHxS and PFOA (Figs. 5 and 2b). However, it is important to highlight that PFOS separation was significantly greater than that of PFHxS or PFOA. This could be due to the greater hydrophobicity and critical micelle formation (CMC) properties of PFOS. It has been shown that surfactants with a lower CMC exhibit better foaming properties and that increasing the hydrophobic chain length of the surfactant lowers its CMC and enhances foamability. [51] Other studies have correlated PFAS separation through foam fractionation with CF_2-chain length and functional head group, showing increased separation for longer-chain PFASs [4,16,19,20]. A cumulative separation of 95 % of

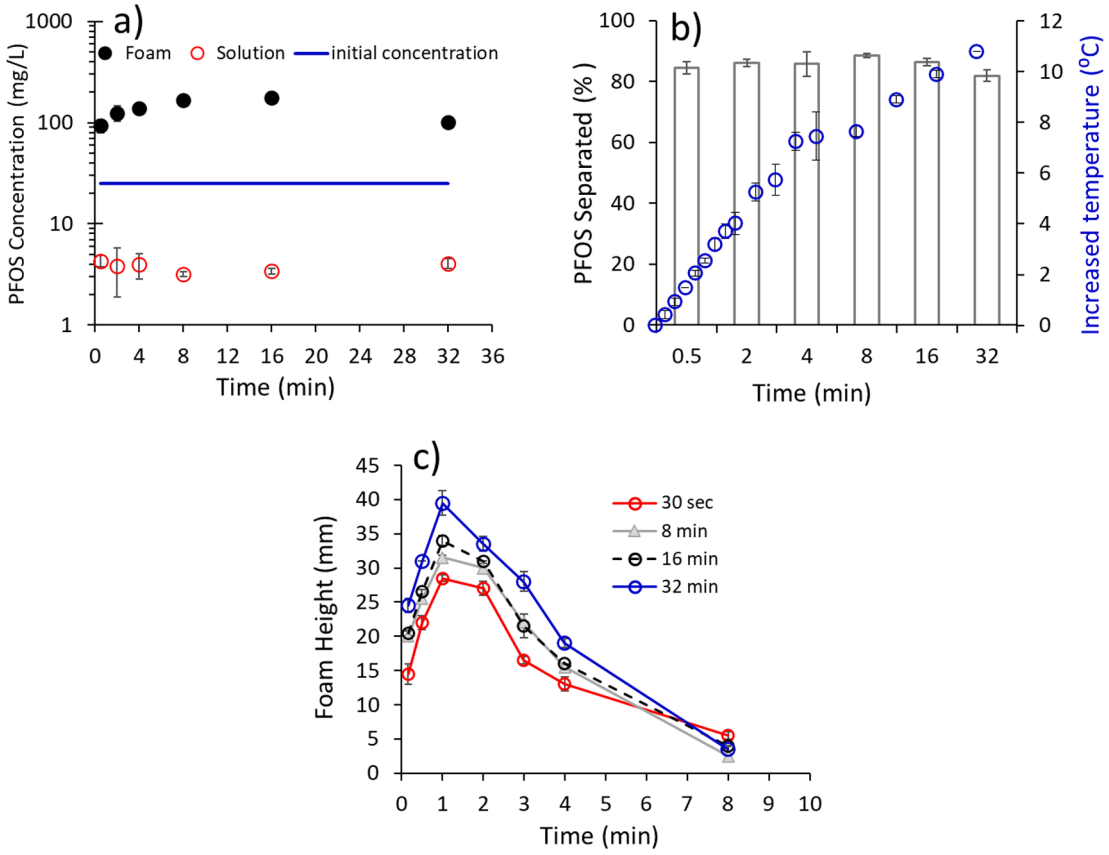

Fig. 4. (a) Concentration of PFOS remaining in the solution and in the foam after mixing a contaminated solution at 6000 rpm for different times, (the blue line is the initial solution concentration" and the red dots are the final solution concentration) (b) Percentage of PFOS mass removed and increase in solution temperature after mixing at different times (the initial solution temperature was the same for all experiments (21.5 ± 0.2 °C), and (c) Foam height measured at different time intervals after mixing a solution for 30 s, 8, 16 and 32 min. Error bars represent standard deviation of n = 3.

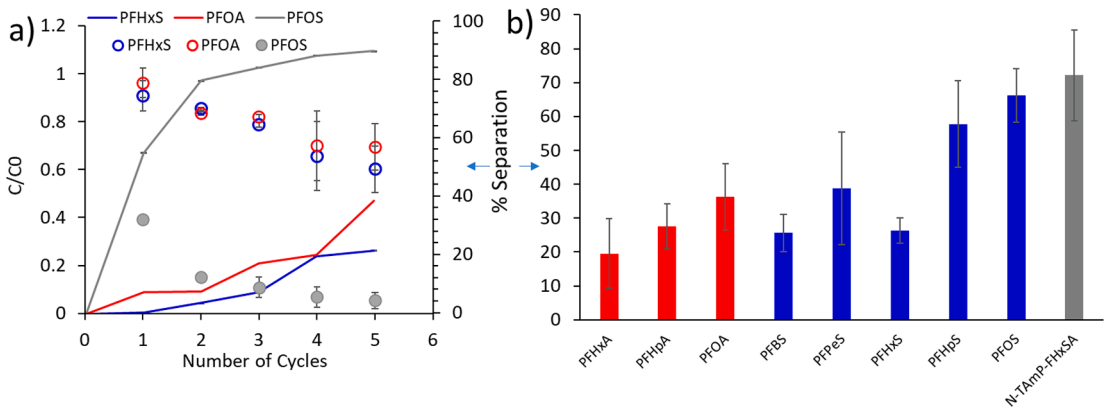

Fig. 5. A) separation of pfos, pfoa and pfhxs over 5 cycles of mixing a spiked solution at 6000 rpm, symbols represent remaining concentration in solution expressed as a fraction of the initial concentration and lines represent % separation, PFAS separation are represented as line while C/C0 as circle dots, and b). Separation efficiencies for various PFASs from a diluted AFFF solution (∑PFASs = 1 mg/L, 6000 rpm, 30 s). Red signifies carboxylate species, blue sulfonate species and grey the zwitterionic species. Error bars representing of standard deviation of n = 3.

the initial PFOS mass was achieved after 5 mixing cycles. Hence, consecutive mixing and foam separation are more effective than long mixing times (Fig. 4c). Mass balances for the PFASs were calculated for each cycle and all PFASs were between 86 to 108 %.

When PFOS concentration was reduced to 1 mg/L, only 27 % of the initial PFOS mass was removed from a solution containing 10 mM NaCl. The volume of foam generated was very low and collapsed quickly. In the solution with 10–15 mg/L concentration of PFOS, the surface tension decreases more than 1 mg/L [52], therefore the water film in the bubble is not pulled back into the liquid water while more bubbles are created [53]. However, when an AFFF solution was used with a ∑PFASs concentration of 1 mg/L (PFOS was the dominant species – 98 %), 66 % of the PFOS mass was removed by a single 30 s cycle (Fig. 5b). PFAS separation was dependent on CF_2-chain length and functional group and a zwitterionic compound (N-TAmP-FHxSA) was more effectively removed than PFOS. This can be related to the effect of surfactant (PFASs) chain length and head group on bubble formation using hydrodynamic cavitation. Leong et al. [54] showed that the zwitterionic surfactant dodecyl dimethyl ammonium propane sulfonate (DDAPS) and Dodecyl trimethyl ammonium chloride (DTAC) caused a greater increase in growth rate than sodium dodecyl sulfate (SDS) or dodecyl dimethyl ammonium propane sulfonate (DDAPS). There were no bubbles formed when 100 μg/L PFOS was subjected to the same mixing conditions. This shows that for lower concentrations of PFASs, co-foaming agents (e.g. surfactants) are required to form CGAs as found in other air- or gas-generated foam fractionation studies [19,20].

3.4. Advantages of the high shear mixing for PFAS separation

Direct comparison of the results of this study with air- or gas generated foam fractionation may not be feasible due to different experimental setups and experiment conditions such as initial feed concentration or addition of co-foaming agents. For example, in the study published by Meng et al [15] that used PFOS at high concentrations (42 mg/L) in a range similar to this study- with or without the addition of co-foaming agents, the authors achieved ~ 99 % PFOS separation after 120 min of aeration. A recent review by We et al. [40] has summarized all of the published results using foam fractionation for PFAS separation where the aeration time used was varied from 20 to 120 min with feed solution concentrations of 1.1 μg/L to 200 mg/L and found varied percentages of PFAS separation from 42 to 99 %. The HSM method described in this study resulted in the separation of 85 % of the PFOS mass within 30 s and more than 95 % in 5 min achieving the separation in a very short time. Similar to other studies that used gas bubble injection for PFAS separation [19,20,40,55], the use of HSM may also require co-foaming agents to remove solutions containing low concentrations of PFASs.

An additional advantage of the method outlined in this paper is its utilisation of off-the-shelf equipment readily available at both laboratory and larger scales. The system could be portable and unlike gas or air-generated foam fractionation, HSM efficient blends and aerate PFAS-contaminated solutions, offering a more straightforward and feasible application under diverse conditions. The simplicity of high shear mixing equipment often translates to lower maintenance costs compared to the foam generation and collection systems utilised in foam fractionation. This technology can serve as a stand-alone method for PFAS separation or be seamlessly integrated into existing treatment processes like adsorption or soil washing.

In general, high shear mixers offer several significant economic advantages across diverse industrial applications such as lower initial investment and operational costs compared to alternative mixing technologies. The simplicity of their design and operation translates to reduced maintenance expenses and less downtime, contributing to overall cost savings. Additionally, high shear mixers are known for their efficiency in achieving rapid and thorough mixing, which leads to shorter processing times and higher throughput. This efficiency not only enhances productivity but also reduces energy consumption, further lowering operational expenses [56]. However, in order to compare high shear mixers with technologies like foam fractionation for PFAS separation, parallel experiments must be conducted under identical conditions to ensure an appropriate comparison.

4. Conclusion

Mixing of PFOS high rotational speed (high shear) conditions can lead to the separation of PFOS via the generation of CGAs due to the surface activity of PFOS. Furthermore, rapid separation of PFOS was achieved (within 30 s) in the presence of a background electrolyte (NaCl) due to the creation of small and stable CGAs. Nevertheless, increasing the mixing rate and time did not affect the transfer of PFOS to the foam. A cumulative separation of 95 % PFOS was achieved after 5 short shear cycles. Separation of PFASs was low for solutions with low concentrations of PFASs (<1 mg/L) which can be potentially resolved by the addition of co-foaming agents, as used for gas- or air generated foam fractionation.

This study demonstrates the substantial potential of PFAS separation from contaminated water using a high shear mixer. The simplicity of this approach could offer economic advantages over the available PFAS separation technologies. Nonetheless, further research is needed to gain a deeper understanding of the phenomenon, enhance its efficiency and

identify its potential and challenges in real-world scenarios such as groundwater or wastewater containing a mixture of PFASs. Improved design should be explored to perform continuous PFAS separation with optimised separation vessel dimensions, mixing rates and times for large-scale separation. Further, a real scenario using groundwater or wastewater containing a mixture of PFASs should be tested.

CRediT authorship contribution statement

Shervin Kabiri: Writing – review & editing, Writing – original draft, Methodology, Investigation, Formal analysis, Data curation, Conceptualization. **Mehdi Jafarian:** Writing – review & editing, Investigation, Formal analysis, Data curation. **Divina A. Navarro:** Writing – review & editing, Investigation. **Catherine P. Whitby:** Writing – review & editing, Validation. **Michael J. McLaughlin:** Writing – review & editing, Validation.

Declaration of competing interest

The authors declare that they have no known competing financial interests or personal relationships that could have appeared to influence the work reported in this paper.

Data availability

Data will be made available on request.

Appendix A. Supplementary material

Supplementary data to this article can be found online at https://doi.org/10.1016/j.seppur.2024.127644.

References

[1] P.R. Kulkarni, D. Aranzales, H. Javed, T.M. Holsen, N.W. Johnson, S.D. Richardson, Mededovic S. Thagard, C.J. Newell, Process to separate per- and polyfluoroalkyl substances from water using colloidal gas aphrons, Remediat. J. n/a (n/a).

[2] Drinking Water Health Advisories for PFOA and PFOS -2022 Interim updated PFOA and PFOS health advisories. America, E. P. A. o. t. U. S. o., Ed. 2022.

[3] PFAS National Environmental Management Plan 2.0. Zealand, H. o. E. o. A. a. N., Ed. 2020.

[4] D.J. Burns, P. Stevenson, P.J.C. Murphy, PFAS removal from groundwaters using surface-active foam fractionation, Remediat. J. 31 (4) (2021) 19–33.

[5] I. Ross, J. McDonough, J. Miles, P. Storch, P. Thelakkat Kochunarayanan, E. Kalve, J. Hurst, S. Dasgupta, J. Burdick, A review of emerging technologies for remediation of PFASs, Remediation 28(2) (2018) 101-126.

[6] B. Cantoni, A. Turolla, J. Wellmitz, A.S. Ruhl, M. Antonelli, Perfluoroalkyl substances (PFAS) adsorption in drinking water by granular activated carbon: Influence of activated carbon and PFAS characteristics, Sci. Total Environ. 795 (2021) 148821.

[7] F. Xiao, Emerging poly-and perfluoroalkyl substances in the aquatic environment: a review of current literature, Water Res. 124 (2017) 482–495.

[8] Treatment technologies and methods for Per- and Polyfluoroalkyl substances (PFAS); Interstate technology regulatory council (ITRC), 2020.

[9] N. Belkouteb, V. Franke, P. McCleaf, S. Köhler, L. Ahrens, Removal of per- and polyfluoroalkyl substances (PFASs) in a full-scale drinking water treatment plant: long-term performance of granular activated carbon (GAC) and influence of flow-rate, Water Res. 182 (2020) 115913.

[10] K.H. Kucharzyk, R. Darlington, M. Benotti, R. Deeb, E. Hawley, Novel treatment technologies for PFAS compounds: a critical review, J. Environ. Manage. 204 (2017) 757–764.

[11] B. Sonmez Baghirzade, Y. Zhang, J.F. Reuther, N.B. Saleh, A.K. Venkatesan, O. G. Apul, Thermal regeneration of spent granular activated carbon presents an opportunity to break the forever PFAS cycle, Environ. Sci. Tech. 55 (9) (2021) 5608–5619.

[12] F. Dixit, R. Dutta, B. Barbeau, P. Berube, M. Mohseni, PFAS removal by ion exchange resins: a review, Chemosphere 272 (2021) 129777.

[13] T.D. Appleman, E.R. Dickenson, C. Bellona, C.P. Higgins, Nanofiltration and granular activated carbon treatment of perfluoroalkyl acids, J. Hazard. Mater. 260 (2013) 740–746.

[14] J.N. Meegoda, B.B. da Souza, M. Monterio Casarini, J.A. Kewalramani, A review of PFAS destruction technologies, Int. J. Environ. Res. Public Health. 19 (24) (2022) 16397.

[15] P. Meng, S. Deng, A. Maimaiti, B. Wang, J. Huang, Y. Wang, I.T. Cousins, G. Yu, Efficient removal of perfluorooctane sulfonate from aqueous film-forming foam solution by aeration-foam collection, Chemosphere 203 (2018) 263–270.

[16] T. Buckley, K. Karanam, X. Xu, P. Shukla, M. Firouzi, V. Rudolph, Effect of mono- and di-valent cations on PFAS removal from water using foam fractionation – a modelling and experimental study, Sep. Purif. Technol. 286 (2022) 120508.

[17] S.J. Smith, K. Wiberg, P. McCleaf, L. Ahrens, Pilot-scale continuous foam fractionation for the removal of Per- and Polyfluoroalkyl substances (PFAS) from landfill leachate, ACS ES&T Water 2 (5) (2022) 841–851.

[18] P. McCleaf, Y. Kjellgren, L. Ahrens, Foam fractionation removal of multiple per- and polyfluoroalkyl substances from landfill leachate, AWWA Water Science 3 (5) (2021) e1238.

[19] T. Buckley, K. Karanam, H. Han, H.N.P. Vo, P. Shukla, M. Firouzi, V. Rudolph, Effect of different co-foaming agents on PFAS removal from the environment by foam fractionation, Water Res. 230 (2023) 119532.

[20] P.H.N. Vo, T. Buckley, X. Xu, T.M.H. Nguyen, V. Rudolph, P. Shukla, Foam fractionation of per- and polyfluoroalkyl substances (PFASs) in landfill leachate using different cosurfactants, Chemosphere 310 (2023) 136869.

[21] S. Hao, P.N. Reardon, Y.J. Choi, C. Zhang, J.M. Sanchez, C.P. Higgins, T. J. Strathmann, Hydrothermal alkaline treatment (HALT) of foam fractionation concentrate derived from PFAS-contaminated groundwater, Environ. Sci. Tech. 57 (44) (2023) 17154–17165.

[22] M. Zupanc, T. Kosjek, M. Petkovšek, M. Dular, B. Kompare, B. Širok, Ž. Blažeka, E. Heath, Removal of pharmaceuticals from wastewater by biological processes, hydrodynamic cavitation and UV treatment, Ultrason. Sonochem. 20 (4) (2013) 1104–1112.

[23] M. Zupanc, T. Kosjek, M. Petkovšek, M. Dular, B. Kompare, B. Širok, M. Stražar, E. Heath, Shear-induced hydrodynamic cavitation as a tool for pharmaceutical micropollutants removal from urban wastewater, Ultrason. Sonochem. 21 (3) (2014) 1213–1221.

[24] G.J. Lye, D.C. Stuckey, Extraction of erythromycin – a using colloidal liquid aphrons: I. Equilibrium partitioning, J. Chem. Technol. Biotechnol.: Int. Res. Process Environ. Clean Technol. 75(5) (2000) 339–347.

[25] P. Jauregi, S. Gilmour, J. Varley, Characterisation of colloidal gas aphrons for subsequent use for protein recovery, Chem. Eng. J. 65 (1) (1997) 1–11.

[26] L. Cabezon, M. Caballero, J. Perez-Bustamante, Coflotation separation for the determination of heavy metals in water using colloidal gas aphrons systems, Sep. Sci. Technol. 29 (11) (1994) 1491–1500.

[27] K. Waters, K. Hadler, J. Cilliers, The flotation of fine particles using charged microbubbles, Miner. Eng. 21 (12–14) (2008) 918–923.

[28] S. Ciriello, S. Barnett, F. Deluise, Removal of heavy metals from aqueous solutions using microgas dispersions, Sep. Sci. Technol. 17 (4) (1982) 521–534.

[29] M.A. Hashim, B.S. Gupta, The application of colloidal gas aphrons in the recovery of fine cellulose fibres from paper mill wastewater, Bioresour. Technol. 64 (3) (1998) 199–204.

[30] D. Roy, K. Valsaraj, W. Constant, M. Darji, Removal of hazardous oily waste from a soil matrix using surfactants and colloidal gas aphron suspensions under different flow conditions, J. Hazard. Mater. 38 (1) (1994) 127–144.

[31] H.J. Couto, G. Massarani, E.C. Biscaia Jr, G.L. Sant'Anna Jr, Remediation of sandy soils using surfactant solutions and foams, J. Hazard. Mater. 164(2-3) (2009) 1325-1334.

[32] M. Duerkop, E. Berger, A. Dürauer, A. Jungbauer, Impact of cavitation, high shear stress and air/liquid interfaces on protein aggregation, Biotechnol. J. 13 (7) (2018) 1800062.

[33] S. Arrojo, Y. Benito, A theoretical study of hydrodynamic cavitation, Ultrason. Sonochem. 15 (3) (2008) 203–211.

[34] P. Jauregi, G.R. Mitchell, J. Varley, Colloidal gas aphrons (CGA): dispersion and structural features, AIChE J 46 (1) (2000) 24–36.

[35] A. Molaei, K.E. Waters, Aphron applications — a review of recent and current research, Adv. Colloid Interface Sci. 216 (2015) 36–54.

[36] J. Cardoso, L. Spinelli, V. Monteiro, R. Lomba, E. Lucas, Influence of polymer and surfactant on the aphrons characteristics: evaluation of fluid invasion controlling, eXPRESS Polym. Lett. 4 (8) (2010).

[37] T.A. Longe, Colloidal gas aphrons: Generation, flow characterization and application in soil and groundwater decontamination, Virginia Polytechnic Institute and State University, 1989.

[38] K. Matsushita, A.H. Mollah, D.C. Stuckey, C. del Cerro, A.I. Bailey, Predispersed solvent extraction of dilute products using colloidal gas aphrons and colloidal liquid aphrons: Aphron preparation, stability and size, Colloids Surf. 69 (1) (1992) 65–72.

[39] C.Y. Tang, Q.S. Fu, A.P. Robertson, C.S. Criddle, J.O. Leckie, Use of reverse osmosis membranes to remove perfluorooctane sulfonate (PFOS) from semiconductor wastewater, Environ. Sci. Tech. 40 (23) (2006) 7343–7349.

[40] A.C.E. We, A. Zamyadi, A.D. Stickland, B.O. Clarke, S. Freguia, A review of foam fractionation for the removal of per- and polyfluoroalkyl substances (PFAS) from aqueous matrices, J. Hazard. Mater. 465 (2024) 133182.

[41] Y.H. Tsang, Y.-H. Koh, D.L. Koch, Bubble-size dependence of the critical electrolyte concentration for inhibition of coalescence, J. Colloid Interface Sci. 275 (1) (2004) 290–297.

[42] D. Nguyen, J. Stults, J. Devon, E. Novak, H. Lanza, Y. Choi, L. Lee, C.E. Schaefer, Removal of per- and polyfluoroalkyl substances from wastewater via aerosol capture, J. Hazard. Mater. 465 (2024) 133460.

[43] A. Koynov, J.G. Khinast, G. Tryggvason, Mass transfer and chemical reactions in bubble swarms with dynamic interfaces, AIChE J 51 (10) (2005) 2786–2800.

[44] C.A. Acuña, J.A. Finch, Tracking velocity of multiple bubbles in a swarm, Int. J. Miner. Process. 94 (3) (2010) 147–158.

[45] X. Ma, M. Li, X. Xu, C. Sun, Coupling effects of ionic surfactants and electrolytes on the stability of bulk nanobubbles, Nanomaterials 12 (19) (2022) 3450.

[46] N. Nirmalkar, A.W. Pacek, M. Barigou, Interpreting the interfacial and colloidal stability of bulk nanobubbles, Soft Matter 14 (47) (2018) 9643–9656.
[47] H. Emami, A. Ayatizadeh Tanha, A. Khaksar Manshad, A.H. Mohammadi, Experimental investigation of foam flooding using anionic and nonionic surfactants: a screening scenario to assess the effects of salinity and pH on foam stability and foam height, ACS Omega 7 (17) (2022) 14832–14847.
[48] S.D. Steffens, E.K. Cook, D.L. Sedlak, L. Alvarez-Cohen, Under-reporting potential of perfluorooctanesulfonic acid (PFOS) under high-ionic strength conditions, Environ. Sci. Technol. Lett. 8 (12) (2021) 1032–1037.
[49] C.E. Schaefer, V. Culina, D. Nguyen, J. Field, Uptake of poly- and perfluoroalkyl substances at the air-water interface, Environ. Sci. Tech. 53 (21) (2019) 12442–12448.
[50] Y. Zhang, A. Sam, J.A. Finch, Temperature effect on single bubble velocity profile in water and surfactant solution, Colloids Surf A Physicochem Eng Asp 223 (1) (2003) 45–54.
[51] S.V. Save, V.G. Pangarkar, Characterisation of colloidal gas aphrons, Chem. Eng. Commun. 127 (1) (1994) 35–54.
[52] J. Costanza, M. Arshadi, L.M. Abriola, K.D. Pennell, Accumulation of PFOA and PFOS at the air-water interface, Environ. Sci. Technol. Lett. 6 (8) (2019) 487–491.
[53] W.R. Smith, Q.X. Wang, The role of surface tension on the growth of bubbles by rectified diffusion, Ultrason. Sonochem. 98 (2023) 106473.
[54] T. Leong, J. Collis, R. Manasseh, A. Ooi, A. Novell, A. Bouakaz, M. Ashokkumar, S. Kentish, The role of surfactant headgroup, chain length, and cavitation microstreaming on the growth of bubbles by rectified diffusion, J. Phys. Chem. C 115 (49) (2011) 24310–24316.
[55] P.R. Kulkarni, D. Aranzales, H. Javed, T.M. Holsen, N.W. Johnson, S.D. Richardson, S. Mededovic Thagard, C.J. Newell, Process to separate per- and polyfluoroalkyl substances from water using colloidal gas aphrons, Remediat. J. 32 (3) (2022) 167–176.
[56] J. Zhang, S. Xu, W. Li, High shear mixers: a review of typical applications and studies on power draw, flow pattern, energy dissipation and transfer properties, Chem. Eng. Process. 57–58 (2012) 25–41.